ACS Chemical Neuroscience

Article

Identification and Profiling of a Selective and Brain Penetrant Radioligand for In Vivo Target Occupancy Measurement of Casein Kinase 1 (CK1) Inhibitors

Travis T Wager, Paul Galatsis, Ramalakshmi Y. Chandrasekaran, Todd W Butler, Jianke Li, Lei Zhang, Scot Mente, Chakrapani Subramanyam, Shenping Liu, Angela C Doran, Cheng Chang, Katherine Fisher, Sarah Grimwood, Joseph R Hedde, Michael Marconi, and Klaas Schildknegt

ACS Chem. Neurosci., **Just Accepted Manuscript** • Publication Date (Web): 13 Jun 2017

ACS Publications

ACS Chemical Neuroscience is published by the American Chemical Society. 1155 Sixteenth Street N.W., Washington, DC 20036

Identification and Profiling of a Selective and Brain Penetrant Radioligand for In Vivo Target Occupancy Measurement of Casein Kinase 1 (CK1) Inhibitors

Travis T. Wager, Paul Galatsis, Ramalakshmi Y. Chandrasekaran, Todd W. Butler, Jianke Li, Lei Zhang, Scot Mente, Chakrapani Subramanyam, Shenping Liu, Angela C. Doran, Cheng Chang, Katherine Fisher, Sarah Grimwood, Joseph R. Hedde, Michael Marconi, Klaas Schildknegt*

Pfizer Worldwide Research and Development: Worldwide Medicinal Chemistry, 1 Portland, Cambridge, MA 02139 and 558 Eastern Point Rd, Groton, CT 06340 (PG, LZ, RYC, TWB, JL, SC, SM, SL, TTW); Pharmacokinetics, Dynamics, and Metabolism, 610 Main Street, Cambridge, MA 02139 and 558 Eastern Point Rd, Groton, CT 06340 (ACD, CC); Internal Medicine Research Unit, 1 Portland, Cambridge, MA 02139 (KF, SG, JRH, MM); Radiochemistry, Pharmaceutical Sciences, 558 Eastern Point Rd, Groton, CT 06340 (KS)

*Tel: 857-225-2840. Fax 860-686-6052. E-mail: travis.t.wager@pfizer.com.

KEYWORDS - Casein kinase 1, CK1, CK1δ/ε, delta, epsilon, kinase inhibitor, circadian rhythm, radiotracer, target occupancy

[a]Abbreviations: ADME, absorption, distribution, metabolism and excretion; AUC, area under the curve; CK1, casein kinase 1; CK1i, Casein Kinase 1 Inhibitor; C_{ave}, average drug concentration;

C_{eff}, efficacious concentration; C_{max}, maximum drug concentration; Cmpd, compound; CNS, central nervous system; circadian rhythm, CR; dark:dark, D:D; HLM, human liver microsomes; Inh, inhibitor; MDR, multi-drug resistance; MPO, multi-parameter optimization; P-gp, P-glycoprotein; SAR, structure-activity relationship; wild type, WT.

Abstract: To enable the clinical development of our CNS casein kinase 1 delta/epsilon (CK1δ/ε) inhibitor project we investigated the possibility of developing a CNS positron emission tomography (PET) radioligand. For this effort, we focused our design and synthesis efforts on the initial CK1δ/ε inhibitor HTS hits with the goal of identifying a compound that would fulfill a set of recommended PET ligand criteria. We identified [^{3}H]PF-5236216 (**9**) as a tool ligand that meets most of the key CNS PET attributes including high CNS MPO PET desirability score and kinase selectivity, CNS penetration and low non-specific binding. We further used [^{3}H]-**9** to determine the binding affinity for PF-670462, a literature CK1δ/ε inhibitor tool compound. Lastly, [^{3}H]-**9** was used to measure in vivo target occupancy (TO) of PF-670462 in mouse and correlated TO with CK1δ/ε in vivo pharmacology (circadian rhythm modulation).

Introduction

A retrospective analysis of historical Pfizer Phase 2 programs led to the 'three pillars of survival' model.[1] In this model, the highest probability of achieving success in clinical studies occurred when the preclinical to clinical translation of the three pillars was met: 1. exposure at the target site of action, 2. binding to the pharmacological target, and 3. expression of pharmacology. For CNS targets, PET ligands are the 'gold standard' for measuring central target engagement (pillar 2) but the identification of suitable PET ligands has been challenging. The identification of PET ligands, until very recently, was one of serendipity. Historically,

compounds identified with the best potency towards the desired target were considered as the most likely radiotracers, while little attention was paid to physicochemical properties, ADME attributes and biological target density (B_{max}). Recently, a rigorous analysis of known PET tracers was undertaken to aid in the rational design and selection of radioligands for in vivo target occupancy measurement. The data from this analysis informed the development of a prospective PET ligand design tool (PET CNS MPO).[2] This set of CNS PET criteria enable a focused compound design with properties best aligned to deliver PET ligands. These criteria coupled with previous understanding around maximum concentration of target binding sites (B_{max}) and binding affinity (K_d) requirement,[3] formed the basis for our radioligand development strategy. Here, we set out to identify a CK1δ/ε selective [^{3}H]-radioligand to: a) provide key brain B_{max} and biodistribution information and inform the probability of the development of a PET tool for this brain kinase target; b) allow for binding affinity and in vivo CK1δ/ε enzyme target occupancy (TO) determination, which in turn could be used to establish a correlation between target occupancy and in vivo circadian rhythm modulation.

Specifically, we set out to identify a radioligand tool compound that would satisfy the following criteria: 1) structurally amenable to [^{3}H] and PET labeling ([^{11}C] or [^{18}F]); 2) physical-chemical properties as defined by CNS PET MPO > 3/6; 3) potent affinity for CK1δ/ε and minimal off-target pharmacology; 4) alignment of ADME attributes (P_{app} AB > 5 x 10^{-6} cm/sec, low transporter liability (Pgp and Bcrp efflux ratio < 2), and good brain availability (AUC $C_{b,u}/C_{p,u} \geq 0.3$); 5) moderate unbound drug fractions in brain and plasma ($F_{u,b}$ > 0.05, $F_{u,p}$ > 0.15). Herein, we report on the key compounds prepared, and the studies used to assess their potential as CK1 target engagement ligands for in vivo target occupancy (TO) tracers and PET tracers.

Results and Discussion

We recently reported the discovery of casein kinase delta and epsilon (CK1δ/ε) inhibitor pyrazolyl-pyridine chemotype **1** in a HTS screening campaign.[4] Structurally, compound **1** was amenable for [^{3}H] and PET radionuclide ([^{11}C] and[^{18}F]) incorporation, thus, represented a viable starting point for target occupancy (TO) radioligand development. Compound **1** was a dual inhibitor of CK1δ and CK1ε that had double-digit nM enzyme affinity for CK1δ (27 nM) and was roughly 5-fold less potent at the structurally related isoform CK1ε (Table 1). Whole cell potency was moderate at 126 nM for CK1δ and 1068 nM for CK1ε. Overall, compound **1** had desirable physical-chemical properties based on the CNS MPO desirability score (4.8/6) and thus had a high probability of having alignment of ADME attributes (Table 1).[5-7] Further, the physical-chemical properties reside in favorable range for PET consideration using the recently disclosed CNS PET MPO desirability tool.[2] However, **1** lacked the desired off-target selectivity profile as it showed potent activity at p38 which resulted in a less than 5-fold selectivity ratio (p38/CK1δ). File mining and medicinal chemistry efforts around **1** led to the discovery and profiling of close-in analogs **2-5** (Table 1). Substitution of the pyridine ring with a methyl group at C2 or C3 (compounds **2** and **3)** lead to a decrease in CK1δ/ε affinity. However, **2** had a modest improvement in selectivity over p38 (9-fold). This result is consistent with previous studies that have shown that substitution at C2 of the pyridine with an amino group induces a peptide flip in the hinge region of p38.[8] Improvement in both potency and selectivity was achieved by incorporating a hydroxyl group on the C2 methyl substituent of **2** to yield **4**. The improvement in selectivity, may be a result of the primary hydroxyl of **4** interacting with the carbonyl of Pro87 of CK1δ, which is not present in p38.[4] Conversion of the primary alcohol of **4** to a methylated amine yielded compound **5**. Compound **5** had similar CK1 inhibitory effects

as **4** and had improved CNS PET MPO desirability score (5.6/6) and p38 selectivity (203 fold). The favorable physicochemical properties improved CK1δ/ε potency and selectivity prompted further profiling and optimization of this chemotype.

Table 1. SAR for CK1 enzyme and whole cell and p38 enzyme

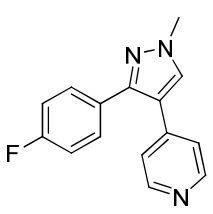

1

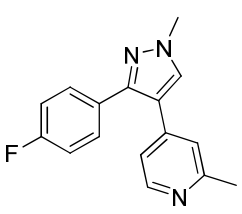

2

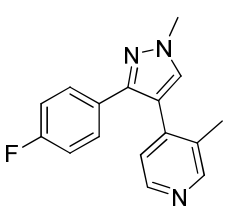

3

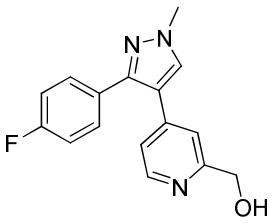

4

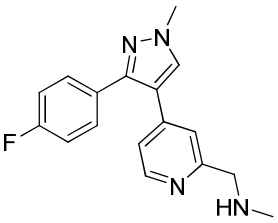

5

Cmpd	CNS MPO (PET MPO) [a]	hCK1δ IC_{50} (nM)[b]	hCK1ε IC_{50} (nM)[b]	hCK1δ EC_{50} (nM)[c]	hCK1ε EC_{50} (nM)[c]	p38 IC_{50} (nM)	P38/ CK1δ
1	4.8 (5.0)	27 (20-35)	126 (107-149)	143 (99-208)	1068 (708-1611)	127 (60-269)	5
2	4.6 (4.9)	37 (n=2)	164 (137-197)	424 (n=1)	ND	340 (n=1)	9
3	4.5 (5.0)	45 (21-91)	203 (140-294)	488 (n=1)	ND	ND	ND
4	5.3 (5.0)	11 (7-17)	68 (48-96)	135 (90-200)	853 (710-1025)	333 (n=1)	29
5	5.8 (5.6)	15 (11-20)	76 (61-95)	45 (28-71)	308 (218-434)	3040 (n=1)	203

[a]Calculated CNS MPO and CNS PET MPO desirability scores were obtained using the published algorithm (maximum value of 6) .[2, 6, 7] Calculated physicochemical properties were obtained using standard commercial packages: BioByte, version 4.3, for ClogP calculations, ACD/Laboratories, version 12.1, for ClogD at pH 7.4, and pKa. [b]Purified human CK1δ and CK1ε in vitro enzymes assays. [c]Human CK1δ and CK1ε mediated PER3 nuclear translocation in cells was measured. Each experiment performed in triplicate, mean S.E.M. and data reported as a mean inhibitory activity with (95% CI) from at least three separate experiments unless otherwise noted.

The next round of design focused on improving potency by rigidifying the molecule and locking it into a bioactive conformation. Substitutions at both C2 and C3 of the pyridine were tolerated and led to the hypothesis that further potency improvements could be achieved by cyclizing the amino group of compound **5** onto the C3 position of the pyridine to yield aza isoindoline **6** (Scheme 1).

Scheme 1. Cyclic amine design strategy

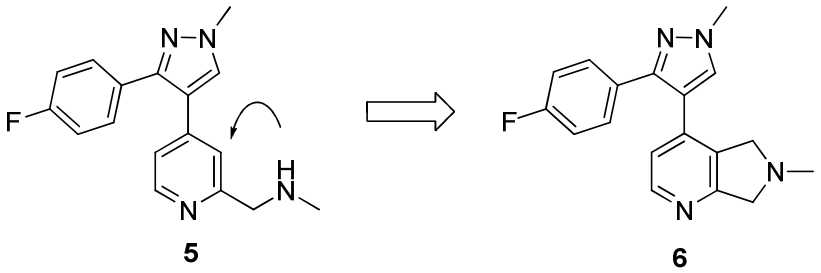

Along the way to the aza isoindoline **6**, key synthetic intermediates were also profiled in the binding, selectivity and ADME assays. The *N*-benzylimide **7** was the first compound included in this profiling and provided a clear indication that the pyridine-dione was not well tolerated (Table 2). This result is not unexpected, in that, the additional carbonyl at the C2 position could lead to an electronic clash with the hinge backbone carbonyl of Leu85. In sharp contrast to **7**, lactam intermediate **8** displayed good CK1δ inhibitory potency (IC_{50} = 8 nM) and selectivity vs. p38 (70 fold). Improved CK1δ/ε potency were observed with the N-methylated lactam **9** (PF-5236216). Compound **9** was the first compound that we identified that exhibited single digit nM potency in the CK1δ enzyme assay (8 nM) and maintained good CK1δ whole cell potency (36 nM) in this series. Importantly, **9** achieved >100-fold selectivity vs. p38 while maintaining an excellent CNS MPO desirability score (6/6) and a PET MPO desirability score (5.5/6). The final targeted compound **6** had a similar CNS PET MPO desirability score as **9**. However, it was less active in the CK1 enzyme assays and whole cell assays**.**

Table 2. SAR for CK1 enzyme and whole cell and p38 enzyme

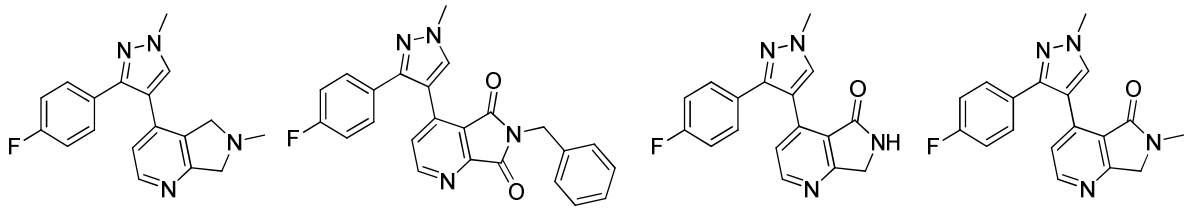

6 7 8 9

Cmpd	CNS MPO (PET MPO) [a]	hCK1δ IC_{50} (nM)[b]	hCK1ε IC_{50} (nM)[c]	hCK1δ EC_{50} (nM)[b]	hCK1ε EC_{50} (nM)[c]	p38 IC_{50} (nM)	P38/ CK1δ
6	5.7 (5.5)	43 (15-118)	232 (113-478)	369 (161-836)	1541 (n=2)	>1884 (n-2)	>44
7	4.2 (2.9)	1677 (853-3299)	>4000	>9000	>10000	ND	ND
8	5.8 (5.9)	10 (9-12)	56 (50-64)	107 (93-123)	630 (567-701)	701 (n=2)	70
9 (PF-5236216)	6.0 (5.5)	8 (7-9)	36 (31-43)	58 (49-68)	318 (282-351)	>861	>114

[a]Calculated CNS MPO and CNS PET MPO desirability scores were obtained using the published algorithm (maximum value of 6).[2, 6, 7] Calculated physicochemical properties were obtained using standard commercial packages: BioByte, version 4.3, for ClogP calculations, ACD/Laboratories, version 12.1, for ClogD at pH 7.4, and pKa. [b]Purified human CK1δ and CK1ε in vitro enzymes assays. [c]Human CK1δ and CK1ε mediated PER3 nuclear translocation in cells was measured. Each experiment performed in triplicate, mean S.E.M. and data reported as a mean inhibitory activity with (95% CI) from at least three separate experiments unless otherwise noted.

To gain a better understanding of the origin of the increased potency and subtype selectivity of **9**, we obtained an X-ray structure of **9** bound to CK1δ (Figure 1). The pyridine ring of **9** forms a single point H-bond acceptor interaction (2.8 Å) with the backbone NH of Leu85 hinge residue. The fluorophenyl group pokes into a hydrophobic pocket that forms adjacent to the

gatekeeper (Met82) residue and also has a favorable stacking interaction between the *p*-fluoro phenyl group and Met82. Presumably, these favorable interactions contributed to the overall improvement in potency and kinome selectivity. The 'free' pyrazole nitrogen of **9** forms a water-mediated H-bond interaction with the conserved Lys38 residue.

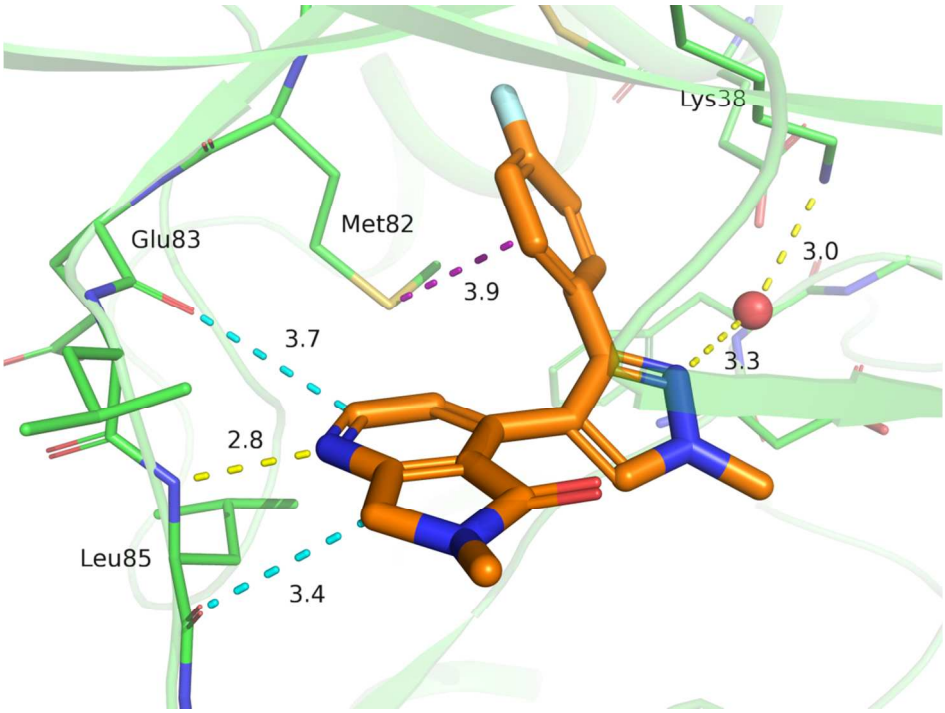

Figure 1. X-ray co-crystal structure showing the binding of CK1δ/ε inhibitor **9** to CK1δ (PDB code INSERT HERE).

From this radioligand-specific SAR effort, **5** and **9** were identified as the best two radioligand leads, and follow-up work was warranted. Compound **5** and **9** were screened in a 100 kinase target promiscuity panel to understand selectivity beyond p38, (Figure 2), see supporting information for more details (Table s1). Four targets were identified as off-target hits for either **5** or **9** at 1 μM, including p38. Follow-up IC_{50} work confirmed ZC3, CK1α, p38 and ZC1 as off-target kinases (Table 3). For both **5** and **9** CK1α was the most active off-target

pharmacology observed with enzyme IC_{50} values of 1059 and 630 nM, respectively. Overall, both compounds exhibited excellent selectivity (≥ 70 fold) in this 100 kinase promiscuity panel.

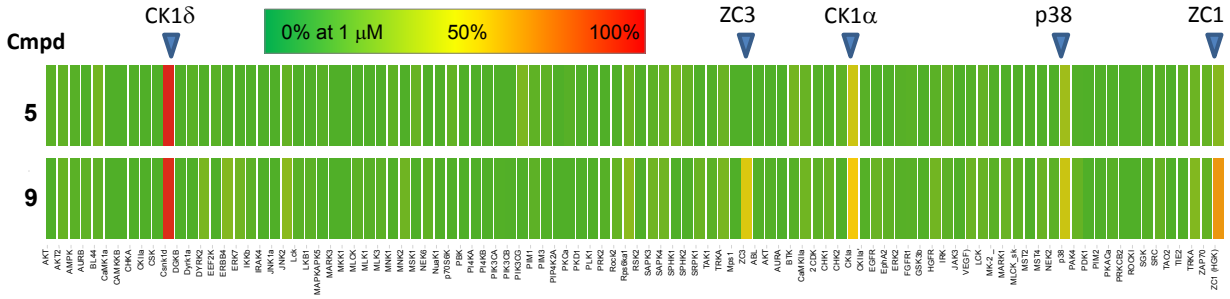

Figure 2. A) Percent inhibition of a 100 kinase target promiscuity panel at 1 μM for compound **5** and **9**. Heat map colors for this continuum: green, 0% inhibition; yellow, 50% inhibition; red, 100% inhibition.

Table 3. Off-target selectivity profiling IC_{50} format and selectivity[a]

Cmpd	Kinase	IC_{50} (nM)	%Inh (1μM)	Selectivity CK1δ/target
5	CK1α	1059	34	71
5	p38	3040	21	203
5	ZC1	>10000	21	>667
5	ZC3	>10200	-1	>680
9	CK1α	630	51	79
9	p38	861	37	108
9	ZC1	873	65	109
9	ZC3	1573	42	197

[a]IC_{50} determination for the four targets hit in the promiscuity panel with inhibition >30% for compound **9**, along with the matched set for compound **5**.

Previously, we demonstrated that ADME attributes are a critical component for the selection of a CNS PET tracer. The set of ADME attributes identified includes passive permeability, transporter liability, fraction unbound drug in plasma and brain compartments and CNS penetration. To further differentiate between **5** and **9** we profiled them in in-vitro and in-vivo

ADME assays. Compound **5** had moderate human liver microsome clearance (HLM) (18 mL/min/mg) and high rat liver microsome clearance (RLM) (64.5 mL/min/mg); in contrast **9** had low HLM and RLM clearance (Table 4). Both compounds had favorable high passive permeability (P_{app} AB > 10 x 10^{-6} cm/sec) values. Transporter liability was higher for **5** (Pgp BA/AB = 2.2 and Bcrp BA/AB = 4.2) than **9** (Pgp and Bcrp BA/AB ≤ 2). The fraction of unbound drug for both **5** and **9** was within an acceptable range (≥ 0.05) in plasma and brain tissue. Lastly, both compounds had good brain penetration as assessed by AUC $C_{b,u}/C_{p,u}$ in mouse. One potential advantage of **9** was that it had significantly higher free brain concentration ($C_{max,b,u}$) at the fixed dose of 56 mg/kg, achieving a free brain concentration of 8685 nM.

Table 4. ADME property summary of for **5** and **9**

Cmpd	HLM[a]	RLM[b]	P_{app}[c]	P-gp[d]	Bcrp[f]	Mouse $F_{u,p}$	Rat $F_{u,b}$	$C_{max,b,u}$ [nM][g]	$AUC_{0-\infty}$ C_b/C_p	$AUC_{0-\infty}$ $C_{b,u}/C_{p,u}$
5	**18**	64.5	17.9	2.2	4.2	0.39	0.09	1480	3.1	0.7
9	**<9**	<39	30	1.2	1.9	0.38	0.24	8685	0.7	0.7

[a]Human liver microsomal clearance (mL/min/mg). [b]Rat liver microsomal clearance (mL/min/mg). [c]Passive permeability (P_{app} AB x 10^{-6} cm/sec) determined by RRCK. [d]Borst MDR1 Efflux Ratio (BA/AB). [f]Mouse Bcrp Efflux Ratio (BA/AB). [g]Mouse $C_{max,b,u}$ values are reported as maximum free drug concentration in brain at a 56 mg/kg dose, s.c.

While both compounds showed favorable properties as radioligand leads, compound **9** was selected for additional evaluation based on slightly better in vitro casein kinase inhibitor (CK1i) potency and higher $F_{u,b}$ to minimize the risk of non-specific binding**.** As shown in Scheme 2, **9** was synthesized using standard alkylation chemistry. Treatment of **8** with [^{3}H]-MeI in the presence of Cs_2CO_3 yielded [^{3}H]-**9** with high specific activity.

Scheme 2. Synthesis of [^{3}H]-9

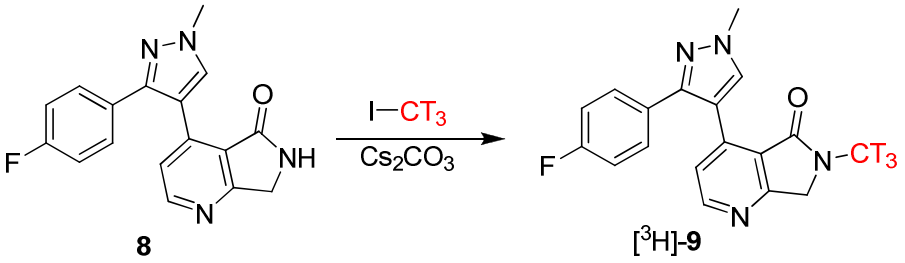

8 [^{3}H]-**9**

Pilot experiments were performed to determine the optimal experimental parameters for performing the in vitro TO, including extract concentrations, relative binding to different brain regions, time and temperature for incubation. Similar to immunolocalization data, CK1δ/ε is expressed throughout the brain with the greatest concentration in the hypothalamus. Saturation binding experiments in the hypothalamus were performed to assess cross-species B_{max} and K_d as shown in Figure 3. CK1δ/ε B_{max} values were comparable between rodent species (rat 12.5 nM and mouse 10.7 nM), but lower in the monkey (6.7 nM). Binding potential (K_d) values were double digit nM (10.2 nM) for rodent species and single digit nM (3.0 nM) in monkey. The B_{max}/K_d ratio was low (<10 fold) for all species with the highest ratio observed in the monkey (2.2 fold). The CK1δ/ε B_{max} (3-5 nM) is in a reasonable range for PET consideration; however, additional potency improvement (i.e. >5 fold) would be necessary to show sufficient specific binding in PET imaging. Continued profiling of the suitability of [^{3}H]-**9** for in vivo TO measurement in rodents was pursued in order to develop a relationship between TO and circadian rhythm activity.

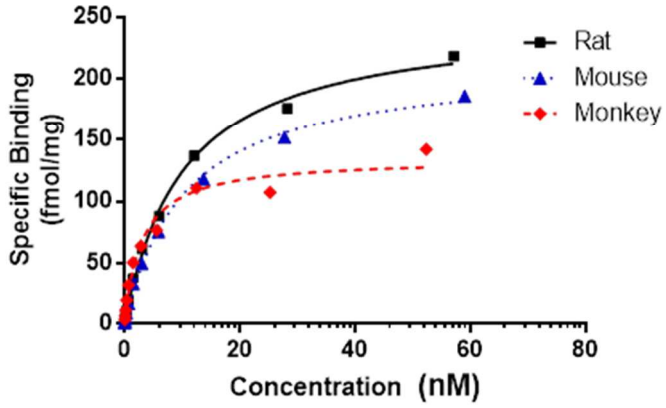

Cmpd	Species	B_{max} (fmol/mg)[a]	B_{max} (nM)[b]	K_d (nM)[a]	B_{max}/K_d
9	Rat	250.2 (236.4-264.9)	12.5	10.2 (8.6-11.7)	1.2
	Mouse	214.2 (198.7-229.6)	10.7	10.4 (8.2-12.6)	1.0
	Monkey	135 (126.0-144.0)	6.7	3.0 (2.3-3.7)	2.2

Figure 3. [a]Saturation [^{3}H]-**9** binding curves for rat, mouse, and monkey brain hypothalamus tissue. Each experiment was performed in triplicate; mean S.E.M. B_{max} and K_d values were determined by GraphPad Prism analyses. [b]B_{max} (fmol/mg) values were converted to nM concentrations assuming 50 mg protein/g wet tissue.[9]

Previously, we reported the in vivo pharmacology of PF-670462 in rodent circadian rhythm models.[10, 11] PF-670462 treatment showed a dose response lengthening of the period in a phase-specific manner and extended the duration of PER2-mediated transcriptional feedback. Using [^{3}H]-**9** we investigated the brain exposure to TO relationship and associated target engagement to the pharmacodynamic response (circadian rhythm phase delay). [^{3}H]-**9** showed a robust specific binding window enabling in-vivo TO studies. A dose-responsive increase in TO was observed for the CK1 inhibitor PF-670462 (Table 5). PF-670462 achieved a 100% TO with a dose of 100 mg/kg (s.c.) and 81% TO with 10 mg/kg (s.c.). The estimated free brain

concentration required to achieve 50% TO of the enzyme was 62 nM and is in line with the whole cell CK1δ inhibitory activity (WC EC_{50} = 58 nM). In general, ≥50% CK1δ/ε in vivo TO resulted in a 2 hr CR phase delay (Figure 4A). Figure 4B is a representative example of the pharmacodynamic response of PF-670462 in mouse after administering 32 mg/kg (s.c., 3 days of dosing). In vivo CR modulation demonstrated expression of CK1i pharmacology (Pillar 3). Together these results enabled us to assess the relationship of target engagement of CK1 inhibitor PF-670462 in brain with the associated pharmacokinetic and pharmacodynamic end points.

Table 5. CK1i brain receptor occupancy from brain binding techniques in mouse for PF-670462 using [^{3}H]-**9**

Compound	Treatment (mg/kg, sc)	$C_{b,u}$ (nM)	Rat CK1δ/ε IVTO (%)[a]
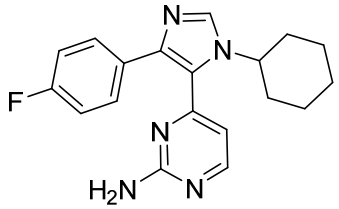 PF-670462	100	1022	100
	10	210	81
	3.2	78	31
	EC_{50}	62 ± 27 nM[b]	

[a]Brain region evaluated: rat hypothalamus (mean ± SEM, *n* = 3–4). Rat in vivo TO analysis with [^{3}H]-**9** and E_{max} fixed at 100%.

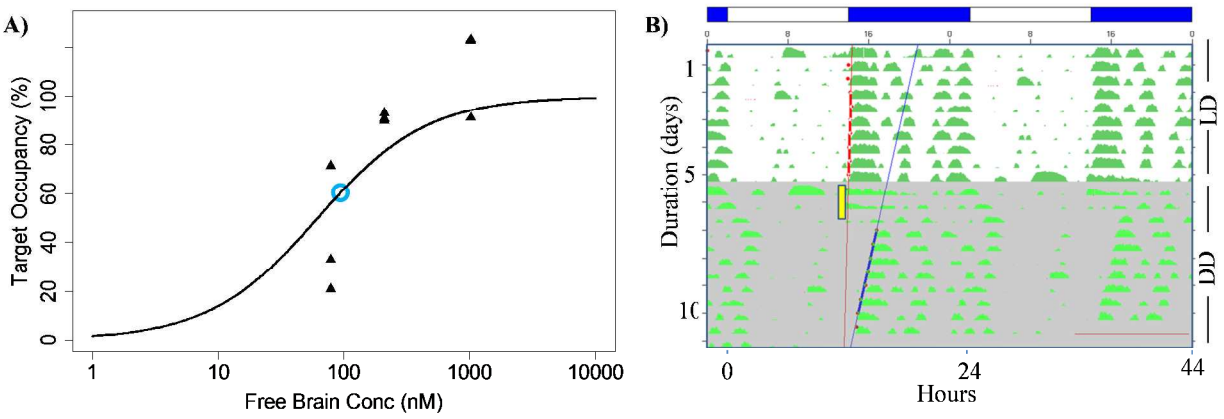

Figure 4. A) Brain region evaluated: rat hypothalamus brain receptor occupancy curves from the in vivo TO protocol in rat. Rat IVTO analysis with [^{3}H]-**9** as tracer and E_{max} fixed at 100%. The black triangle data points represent actual measured TO and brain PK from individual animals. The solid line is the data-fitted TO model. The blue circle represents exposure, C_{ave} (over 4hrs) and TO (67% IVTO) to yield a 4 hr phase shift in dark: dark (D:D) mouse in vivo circadian rhythm model (32 mg/Kg s.c. after 3-days dosing of PF-670462). B) Representative scaled temperature actograms for PF-670462 reveal significant period lengthening by PF-670462 in WT animals after 3 d of dosing, previously reported. The phase shift depicted was -3.70 hours following dosing for 3 days in DD.

Conclusions

As part of our clinical development strategy for the CK1i program, we investigated the possibility of developing a CNS PET tracer. For this effort we leveraged the initial CK1i HTS hits to fuel our design and synthesis plans with the goal of identifying a compound that would fulfill a set of recommended PET ligand design criteria, Table 5. In the initial triage of potential starting points, we focused on the N-methyl pyrazole chemotype in part due to ease of incorporating a [^{3}H] and [^{11}C] labels. Initial SAR yielded amine **5** that had a double digit IC_{50} for CK1δ and was over 100 fold selective for CK1 over other kinases. Additional SAR work yielded a novel synthetic intermediate **9** that was single digit IC_{50} for CK1δ and greater than 70

fold selective over related CK1α isoform. The physicochemical properties of **9** were in favorable range for a PET ligand (CNS PET MPO > 3/6) with an overall CNS PET MPO desirability score of 5.5/6. Consistent with high passive permeability and low transporter liabilities (Pgp and Bcrp), brain penetration was excellent (mouse AUC $C_{b,u}/C_{p,u}$ = 0.7). Using $F_{u,b}$ as a surrogate for non-specific binding, **9** was predicted to have low non-specific binding and was confirmed in vivo using [^{3}H]-**9**. Using [^{3}H]-**9** saturation curves for rat, mouse, and monkey for brain hypothalamus tissue, experimental $B_{max,}$ and K_d values were determined. In monkey, the B_{max} and K_d values were 6.7 nM and 3.0 nM, respectively and a B_{max}/K_d ratio of 2.2. While **9** does not meet the B_{max}/K_d criteria for CNS PET ligand development, it proved to be instrumental in generating a fundamental understanding of TO to free brain concentration for the CK1i tool compound PF-670462 (EC_{50} = 62 nM). Further, [^{3}H]-**9** was used to connect TO and the CR behavioral output (Pillar 3).[1] In an in vivo CR model a 32 mg/kg s.c. dose yielded a free brain exposures sufficient to occupy 67% of the CK1 enzyme which resulted in a 3.7 hr phase shift. Further work will be required to improve CK1 potency (~5 fold) while retaining the desirable PET attributes of **9** to identify a CNS PET ligand.

Table 5. Summary of CNS PET attributes for **9.**

Property	Attribute	Target Value	Value[a]
Physicochemical Properties	PET MPO	>3	5.5
Synthetic Enabled Label Sites	[^{3}H], [^{11}C], [^{19}F]	1 site	2 sites
Brain Permeability	P_{app}	> 10	30
	MDR ER	≤ 2.5	1.2
	Bcrp ER	≤ 2.5	1.9
	$C_{b,u}/C_{p,u}$	≥ 0.3	0.7
Non-specific Binding	$F_{u,p}$	≥ 0.15	0.38
	$F_{u,b}$	≥ 0.05	0.24
	$F_{u,b}$ and $F_{u,p}$	≥ 0.15 and ≥ 0.05	Yes
Pharmacology	Selectivity	>30x	>70x

B_{max}/K_d	$\geq$ 10x	2.2	

[a]Color code: red, fail to meet target value and green, meet target value.

Chemistry

The preparation of compounds **6-9** is outlined in Scheme 3. Suzuki coupling of 3-fluoro-4-iodopicolinonitrile with pinacol boronate **10**[4] proceeded in modest yield to give the diarylated pyrazole **11**. Treatment of **11** with potassium cyanide afforded the dinitrile **12** via SNAr displacement in quantitative yield. The nitriles were then hydrolyzed with 5N aqueous potassium hydroxide at 100 °C. Upon cooling, the dipotassium salt of the diacid product **13** precipitated from solution allowing for isolation via filtration. Refluxing the diacid salt in a 1:1 mixture of acetic anhydride and acetic acid gave the phthalic anhydride **14** which was isolated after concentration by trituration with diethyl ether. This material was used without further purification due to its reactivity with water and instability on silica gel. Compounds **7**, **15** and **16** were accessed by the addition of primary amines into the anhydride and then subsequent in situ ring closure using acetic acid/acetic anhydride. Selective reduction of the less hindered carbonyl with zinc dust in hot acetic acid yielded the lactams **8** and **9**.

Scheme 3. Synthesis of 7, 8, and 9[a]

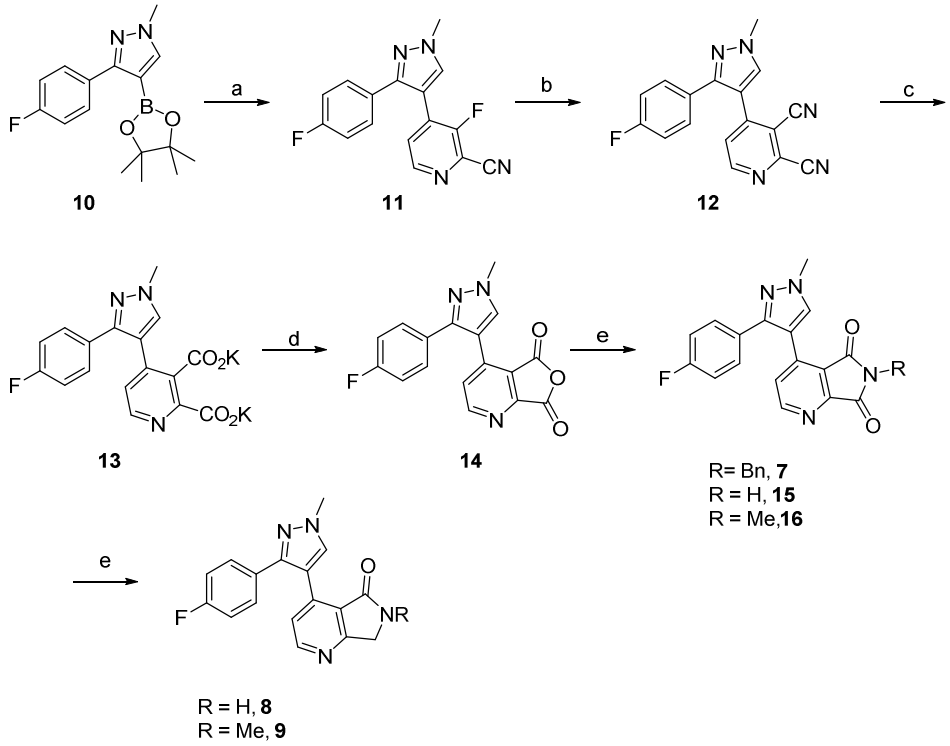

[a]Reagents and Conditions: (a) 3-fluoro-4-iodopicolinonitrile, 1.2 equiv of Cs_2CO_3, DMF, $Pd_2(dba)_3$, 50 °C, 6 h (59%); (b) KCN, DMSO, 50 °C, 2 h (quant.); (c) 5N aq KOH, 100 °C, 24 h (88%); (d) Ac_2O, HOAc, THF, 110 °C, 3 h; (e) Ac_2O, HOAc, $BnNH_2$ (**7**, 75%), or NH_4OH (**15**, 92%) or $MeNH_2$ (**16**, 93%), 80-120 °C, 2 h; (f) 5 equiv of Zn dust, HOAc, 110 °C, 1.5-4.5 h, (**8**, 41%),(**9**, 53%)

Azaisoindoline **6** was prepared as outlined in Scheme 4. Protection of azaisoindoline **17** as the sulfonamide **18** was achieved by treatment with methanesulfonyl chloride. N-oxide **19** was prepared via mCPBA oxidation. Chlorination with oxalyl chloride gave the desired regioisomer **20** in 44% yield with 14% of the corresponding 2-chloro isomer which was readily separated by chromatography. Suzuki coupling with pinacol boronate **10** afforded the protected azaisoindoline template **21**. Cleavage of the methylsulfonamide in a 1:1 mixture of refluxing 48% hydrobromic acid and acetic acid provided the unprotected azaisoindoline **22**. Subsequent reductive amination

with aqueous formaldehyde and sodium triacetoxyborohydride cleanly yielded the N-methylated product **6**.

Scheme 4. Synthesis of 6[a]

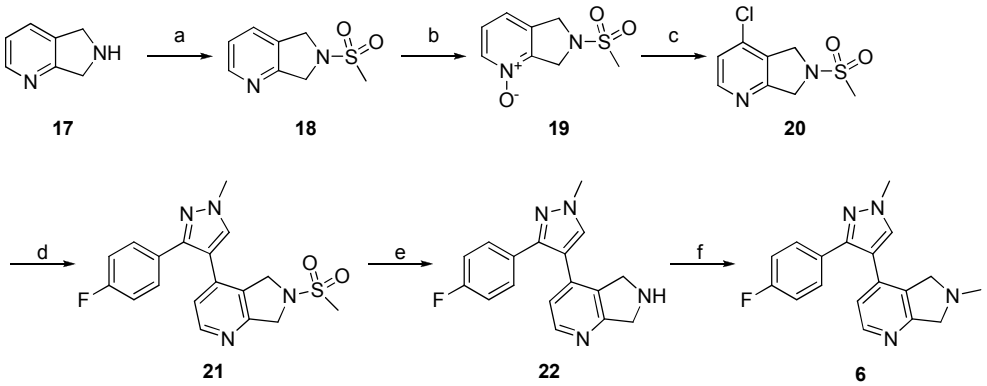

[a]Reagents and Conditions: (a) methanesulfonyl chloride, DIPEA, methylene chloride, -10 °C to rt, 18 h (quant.); (b) 2 equiv of mCPBA, methylene chloride, rt, 20 h (95%); (c) oxalyl chloride, DMF, rt, 18 h (44%); (d) 1.2 equiv of **10**, 3 equiv of LiOH, DMF, 4 mol% of $Pd(dppf)Cl_2$, 100 °C, 2 h (59%); (e) 48% aq. HBr, HOAc, reflux, 18 h (63%); (f) 37% aq. formaldehyde, methylene chloride, STAB, rt, 18 h (73%)

Experimental section

General Information. All solvents and reagents were obtained from commercial sources and were used as received. All reactions were followed by TLC (TLC plates F254, Merck) or LCMS (liquid chromatography−mass spectrometry) analysis. Varian 300, 400, or 500 MHz instruments were used to obtain ^{1}H and ^{13}C NMR spectra in deuterated solvents. All proton shifts are reported in δ units (ppm) and were measured relative to signals for chloroform (7.27 ppm), methanol (3.31 ppm) or deuterium oxide (4.75 ppm). All ^{13}C shifts are reported in δ units (ppm) relative to the signals for chloroform (77.0 ppm) or methanol (49.2 ppm) with ^{1}H decoupling. All coupling constants (J values) are reported in hertz (Hz). GCMS were recorded on an HP 6890 GC system equipped with a 5973 mass selective detector (stationary phase, HP-1, fused silica, 12

m × 0.202 mm × 0.33 μm; temperature limits, −60 to 325 °C; ramp rate = 30 °C/min; solvent delay = 0.4 min). Analytical analyses by UPLC were performed on a Waters Acquity system with PDA detection (UV 210 nm) at 45 °C and flow rate 0.5 mL/min, with a gradient of 95/5 buffer/acetonitrile (0−7.55 min), 10/90 buffer/acetonitrile (7.55−7.85 min), 95/5 buffer/acetonitrile (8.10−10.30 min) using the following columns and buffers: Waters BEH C8 column (2.1 × 100 mm, 1.7 um) with 50 mM sodium perchlorate/0.1% phosphoric acid or 10 mM ammonium bicarbonate as buffer; Waters BEH RP C18 column (2.1 × 100 mm, 1.7 um) or Waters HSS T3 (2.1 × 100 mm, 1.8 um) column with 0.1% methanesulfonic acid buffer. Mass spectra were recorded on a Micromass ADM atmospheric pressure chemical ionization instrument (MS, APCI). High-resolution mass spectra were obtained on an Agilent 6620 LC-MS TOF equipped with a Zorbax Eclipse column (50 mm × 4.6 mm, 1.8 μm XDB-C18) using 0.1% formic acid aqueous as mobile phase A1 and acetonitrile containing 0.1% formic acid as mobile phase B1. Column chromatography was carried out on silica gel 60 (32−60 mesh, 60 Å) or on prepacked Biotage or ISCO columns. The purities of final compounds **6-9** as measured by UPLC were found to be above 95%.

3-Fluoro-4-(3-(4-fluorophenyl)-1-methyl-1H-pyrazol-4-yl)picolinonitrile (11). 3-(4-Fluorophenyl)-1-methyl-4-(4,4,5,5-tetramethyl-1,3,2-dioxaborolan-2-yl)-1H-pyrazole (**10**)[4] (14.5 g, 48.0 mmol) and 3-fluoro-4-iodopicolinonitrile (9.92 g, 40.0 mmol) were combined in 100 mL DMF and treated with Cs_2CO_3 (19.90 g, 61.2 mmol). The resulting suspension was sparged with nitrogen for 20 min and treated with tris(dibenzylideneacetone)dipalladium(0) (1.51 g, 1.6 mmol) in a single portion. The nitrogen sparging was continued for an additional 20 min, and stirring of the dark suspension was continued for 30 min at rt. The reaction mixture was warmed to 50 ºC for 6 h and was allowed to cool to rt overnight. The thick slurry was added to 150 mL

EtOAc, the suspension was diluted with 50 mL 50% saturated aqueous sodium chloride, treated with decolorizing carbon, and stirred 1h at rt. The mixture was filtered through celite, the layers were separated, and the organic layer was washed with 3 x 30 mL 50% saturated aqueous NaCl. The organic layer was dried over anh. $MgSO_4$ and was concentrated in vacuo to give 18 g of a pasty orange solid. The solid was dissolved in a minimum amount of methylene chloride, loaded onto a 100 g SNAP cartridge, and the crude material was eluted over a 340 g SNAP cartridge with a 5-80% EtOAc/heptane gradient over 4.8 L. The appropriate fractions were combined and concentrated. During concentration, a white solid precipitated. This was collected to give 6.93 g (59%) of the title compound product as a white solid. APCI MS m/z 297.0 (M+1). ^{1}H NMR ($CDCl_3$, 400 MHz,): δ 8.28 (d, *J* = 5.1, 1H), 7.84 (d, *J* = 2.9, 1H), 7.40 (dd, *J* = 5.3, 2.2, 2H), 7.25 (dd, *J* = 5.8, 4.9, 1H), 7.09 (dd, *J* = 8.6, 8.6, 2H), 4.02 (s, 3H). HRMS: calcd for $C_{16}H_{10}F_2N_4$ 297.0946 $(M + H)^+$, found 297.0941.

4-(3-(4-Fluorophenyl)-1-methyl-1H-pyrazol-4-yl)pyridine-2,3-dicarbonitrile (12). Fluorocyanopyridine **11** (10.00 g, 33.8 mmol) was dissolved in DMSO (100 mL) with gentle heating. Potassium cyanide (2.35 g, 35.0 mmol) was added and the mixture was heated to 50 ºC and stirred. After 2 h, the reaction was cooled in an ice bath and 0.1N aqueous NaOH (50 mL) was added. The resulting slurry was stirred for 5 min, the solids were collected, rinsed with water and air-dried to yield 10.34 g (quant) of the title compound as a light cream colored solid. ^{1}H NMR ($CDCl_3$, 400 MHz,): δ 8.56 (d, *J* = 5.2, 1H), 8.02 (s, 1H), 7.33 (dd, *J* = 8.9, 5.2, 2H), 7.24 (d, *J* = 5.5, 1H), 7.06 (dd, *J* = 8.6, 8.6, 2H), 4.02 (s, 3H). HRMS: calcd for $C_{17}H_{10}FN_5$ 304.0993 $(M + H)^+$, found 304.0991.

4-(3-(4-Fluorophenyl)-1-methyl-1H-pyrazol-4-yl)pyridine-2,3-dicarboxylic acid, dipotassium salt (13). Pyridinedinitrile **12** (10.34 g, 34.1 mmol) and aqueous KOH (28.3 g, 504

mmol, dissolved in 100 mL water) were heated at 100 ºC for 24 h. The mixture was cooled in ice to give a thick white slurry. The material was warmed back to rt, filtered and air dried to yield 12.47 g (88%) of the title compound as a cream colored solid. LCMS m/z 342.1 (M+1). ^{1}H NMR (D_2O, 400 MHz,): δ 8.15 (*d*, *J* = 5.1, 1H), 7.77 (s, 1H), 7.39 (dd, *J* = 9.0, 5.5, 2H), 7.08 (dd, *J* = 9.0, 9.0, 2H), 6.99 (d, *J* = 5.1, 1H), 3.92 (s, 3H).

4-(3-(4-Fluorophenyl)-1-methyl-1H-pyrazol-4-yl)furo[3,4-b]pyridine-5,7-dione (14). Diacid **13** (5.00 g, 12.0 mmol) was slurried with acetic acid (35 mL) and acetic anhydride (12.5 mL) and heated to 110 ºC for 3h. The resulting homogeneous mixture was cooled and concentrated, slurried with 50 mL diethyl ether and re-concentrated to yield the title compound as a sticky yellow solid. This material was used without purification in the next step. An analytical sample was purified by chromatography (ISCO 12g, heptane/EtOAc 6/4 to 0/1 in 10 min) to give a white solid. GCMS m/z 323.0 (M). ^{1}H NMR ($CDCl_3$, 400 MHz,): δ 8.78 (d, *J* = 5.3, 1H), 8.30 (s, 1H), 7.41 (dd, *J* = 8.8, 5.3, 2H), 7.34 (d, *J* = 5.3, 1H), 7.11 (dd, *J* = 8.6, 8.6, 2H), 4.08 (s, 3H).

6-Benzyl-4-(3-(4-fluorophenyl)-1-methyl-1H-pyrazol-4-yl)-5H-pyrrolo[3,4-b]pyridine-5,7(6H)-dione (7). Phthalic anhydride **14** (472 mg, 1.46 mmol) and benzyl amine (0.167 mL, 1.53 mmol) in acetic acid (4.7 mL) were heated at reflux for 18 h, cooled and then concentrated to a brown solid. This material was stirred with diethyl ether (20 mL) for 10 min and then filtered to yield 450 mg (75%) of title compound as a tan colored solid. LCMS m/z 413.5 (M+1). ^{1}H NMR ($CDCl_3$, 400 MHz,): δ: 8.57 (d, *J* = 5.2, 1H), 8.15 (s, 1H), 7.26-7.42 (m, 7H), 7.13 (d, *J* = 5.3, 1H), 7.01 (dd, *J* = 8.6, 8.6, 2H), 4.87 (s, 2H), 4.00 (s, 3H). ^{13}C NMR ($CDCl_3$, 100 MHz): δ 166.4, 165.6, 162.8 (d, J_{F-C} = 248.1), 153.8, 152.8, 150.1, 139.9, 135.8, 134.4, 130.2 (d, J_{F-C} =

8.1), 128.6-128.5 (m, doublet and two singlets overlapping), 127.9, 127.8, 122.1, 115.7 (d, J_{F-C} = 21.4), 111.8, 41.7, 39.3. HRMS: calcd for $C_{24}H_{17}FN_4O_2$ 413.1408 $(M + H)^+$, found 413.1408.

4-(3-(4-fluorophenyl)-1-methyl-1H-pyrazol-4-yl)-5H-pyrrolo[3,4-b]pyridine-5,7(6H)-dione (15). Phthalic anhydride **14** (190 mg, 0.588 mmol) and 28-30% aqueous ammonium hydroxide (4 mL) were heated to a vigorous reflux for 30 min and then concentrated. The residue was dissolved in 1:1 acetic acid/acetic anhydride (20 mL) and heated at 120 ºC for 2hr and concentrated. The residue was dissolved in EtOAc and run through a short silica gel plug to afford 176 mg (92%) of title compound as a white solid which was used without further purification. LCMS m/z 323.1 (M+1). ^{1}H NMR (MeOH-d_4, 400 MHz,): δ 8.62 (d, *J* = 5.3, 1H), 8.26 (s, 1H), 7.42 (dd, *J* = 9.0, 5.3, 2H), 7.27 (d, *J* = 5.3, 1H), 7.10 (dd, *J* = 9.0, 9.0, 2H), 4.02 (s, 3H).

4-(3-(4-Fluorophenyl)-1-methyl-1H-pyrazol-4-yl)-6-methyl-5H-pyrrolo[3,4-b]pyridine-5,7(6H)-dione (16). Phthalic anhydride **14** (275.3 g, 659.4 mmoles), acetic acid (2.06 L) and acetic anhydride (138 mL, 1456 mmol) were heated at 110 ºC for 1 hr, cooled to 80 ºC and then methylamine (2.0M/THF, 659 mL; 567.1 g) was added over 20 min, maintaining the temperature at 80 ºC. A white smoke was observed during the addition. The reaction was heated to 100 ºC overnight and concentrated to approximately 500 mL giving a clear yellow solution. Water (200 mL) was added over 10 min with stirring. Acetic acid (~ 100 mL) and an additional 200 mL of water were added to aid stirring. The solids were removed by filtration using a Buchner funnel with cloth and washed with 250 mL water. The material was air dried for 1h then dried in a vacuum oven at 60 ºC overnight to yield 206.5 g (93.1%) of title compound as a light yellow solid. LCMS m/z 337.1 (M+1). ^{1}H NMR ($CDCl_3$, 400 MHz,): δ 8.61 (d, *J* = 5.5, 1H), 8.22 (s,

1H), 7.41 (dd, *J* = 9.0, 5.5, 2H), 7.1 (d, *J* = 5.3, 1H), 7.07 (dd, *J* = 8.8, 8.8, 2H), 4.05 (s, 3H), 3.26 (s, 3H). HRMS: calcd for $C_{18}H_{14}FN_4O_2$ 337.1095 $(M + H)^+$, found 337.1093.

4-(3-(4-fluorophenyl)-1-methyl-1H-pyrazol-4-yl)-6,7-dihydro-5H-pyrrolo[3,4-b]pyridin-5-one (8). Phthalimide **15** (176 mg, 0.55 mmol) and zinc dust (178 mg, 2.73 mmol) in glacial acetic acid (2.4 mL) were heated at 110 °C for 1.5h. After cooling, the mixture was filtered through celite with HOAc rinse and concentrated to yield a sticky orange solid. Silica gel chromatography using a 100% methylene chloride to 10% MeOH/ methylene chloride gradient over 10 min gave the title compound (120 mg, 71%) as a white solid. LCMS m/z 309.1 (M+1). ^{1}H NMR ($CDCl_3$, 400 MHz): δ 8.40 (d, *J* = 5.4, 1H), 8.21 (s, 1H), 7.37-7.49 (m, 2H), 6.95-7.03 (m, 3H), 6.14 (br s, 1H), 4.74 (s, 2H), 3.98 (s, 3H). ^{13}C NMR (MeOH-d_4, 100 MHz): δ 171.1, 167.1, 164.3 (d, J_{F-C} = 246.5), 152.7, 151.0, 142.3, 136.4, 131.7 (d, J_{F-C} = 8.8), 130.7 (d, J_{F-C} = 3.8), 126.0, 123.7, 116.6 (d, J_{F-C} = 22.0), 114.2, 47.7, 39.3. HRMS: calcd for $C_{17}H_{13}FN_4O_2$ 309.1146 $(M + H)^+$, found 309.1144.

4-[3-(4-Fluorophenyl)-1-methyl-1H-pyrazol-4-yl]-6-methyl-6,7-dihydro-5H-pyrrolo[3,4-b]pyridin-5-one (9). To a flask equipped with overhead stirring was added **16** (202.0 g, 600.6 mmoles) and zinc dust (<10 micron) (357.0 g, 5.41 moles) followed by acetic acid (2.02 L). The mixture was heated to 105 ºC and stirred for 4.5 hr, then cooled to rt. Celite was added to the reaction mixture, and this was filtered to remove the zinc The filter pad was rinsed with EtOAc and the filtrate was concentrated to ~ 300 mL, then 200 mL of water was added. The resulting solid was collected, rinsed with water, and dried under vacuum overnight to give 103.2 g (53%) of the title compound as a solid. LCMS m/z 323.2 (M+1). ^{1}H NMR ($CDCl_3$, 400 MHz): δ 8.38 (d, *J* = 5.5, 1H), 8.28 (s, 1H), 7.41 (dd, *J* = 8.8, 5.5, 2H), 7.03 (dd, *J* = 8.6, 8.6, 2H), 6.96 (d, *J* = 5.2, 1H), 4.44 (s, 2H), 4.01 (s, 3H), 3.24 (s, 3H). ^{13}C NMR (MeOH-d_4, 100 MHz): δ 165.2, 164.5

(d, J_{F-C} = 247.4), 159.1, 152.1, 150.0, 142.2, 138.9, 131.9 (d, J_{F-C} = 8.8), 129.5 (d, J_{F-C} = 3.0), 127.0, 126.9, 116.9 (d, J_{F-C} = 22.1), 112.4, 50.7, 39.5, 29.7. HRMS: calcd for $C_{18}H_{15}FN_4O$ 323.0508 $(M + H)^+$, found 323.1298.

6-(Methylsulfonyl)-6,7-dihydro-5H-pyrrolo[3,4-b]pyridine (18). Methanesulfonyl chloride (0.97 mL, 12.4 mmol) was added dropwise to a -10 ºC solution of diisopropyl-ethylamine (5.16 mL, 31.1 mmol) and **17** (2.0 g, 10.0 mmol) in methylene chloride (20 mL). The mixture was stirred overnight at rt, diluted with methylene chloride (300 mL) and washed with saturated aqueous sodium bicarbonate. The organic phase was separated, dried ($MgSO_4$) and filtered through a short silica gel pad with EtOAc rinse. The filtrate was concentrated to yield 2.15 g (quantitative) of title compound as a solid which was used without further purification. LCMS m/z 199.2 (M+1). ^{1}H NMR ($CDCl_3$, 400 MHz): δ 8.54 (d, J = 4.9, 1H), 7.61 (d, J = 7.8, 1H), 7.25 (dd, J = 7.8, 5.1, 1H), 4.75 (AB quartet, J_{AB} = 2.1, $\Delta\nu_{AB}$ = 7.8, 4H), 2.94 (s, 3H). HRMS: calcd for $C_8H_{10}N_2O_2S$ 199.0536 $(M + H)^+$, found 199.0530.

6-(Methylsulfonyl)-6,7-dihydro-5H-pyrrolo[3,4-b]pyridine 1-oxide (19). *m*-Chloroperbenzoic acid (70% purity, 2.94 g, 11.9 mmol) was added to a solution of **18** (2.15 g, 10.84 mmol) in methylene chloride (43 mL). After 2h a gummy solid had formed and LCMS showed ~50 % conversion. Chloroform (20 mL) was added to help solubility and an additional equivalent of *m*-chloroperbenzoic acid (2.8 g) was added and the stirring was continued for another 18h at rt to drive the reaction to completion. The crude reaction mixture was loaded onto a silica gel plug, flushed with EtOAc (500 mL- discarded) and then eluted with 50% MeOH/EtOAc (2L) to give the desired product. Concentration yielded the title compound (2.22 g, 95%) as a white solid. LCMS m/z 215.0 (M+1). ^{1}H NMR ($CDCl_3$, 400 MHz): δ 8.16 (d, J = 6.5, 1H), 7.29 (dd, J = 7.5,

7.5, 1H), 7.18 (d, *J* = 7.8, 1H), 4.82-4.89 (m, 4H), 2.96 (s, 3H). HRMS: calcd for $C_8H_{10}N_2O_3S$ 215.0485 $(M + H)^+$, found 215.0480.

4-Chloro-6-(methylsulfonyl)-6,7-dihydro-5H-pyrrolo[3,4-b]pyridine (20). Oxalyl chloride (0.415 mL, 4.67 mmol) was added dropwise to a 0 ºC suspension of **19** (500 mg, 2.33 mmol) in DMF (40 mL). The resulting mixture was warmed to rt and stirred for 18 hr. Water was added slowly to quench the excess oxalyl chloride and the mixture was extracted into methylene chloride (250 mL). The extract was washed with brine, dried ($MgSO_4$) and concentrated to yield a brown gum which was then purified by silica gel chromatography using a heptanes (100%) to 50% EtOAc/heptanes gradient. Regioisomer 2-chloro-6-(methylsulfonyl)-6,7-dihydro-5H-pyrrolo[3,4-b]pyridine (76 mg, 14%) eluted from the column first followed by the desired title compound (240 mg, 44%, white solid). ^{1}H NMR ($CDCl_3$, 400 MHz): δ 8.45 (d, *J* = 5.5, 1H), 7.26 (d partially obscured by residual $CHCl_3$ peak, 1H), 4.80 (br s, 4H), 2.97 (s, 3H). HRMS: calcd for $C_8H_9ClN_2O_2S$ 233.0146 $(M + H)^+$, found 233.0143.

4-[3-(4-fluorophenyl)-1-methyl-1H-pyrazol-4-yl]-6-(methylsulfonyl)-6,7-dihydro-5H-pyrrolo[3,4-b]pyridine (21). 20 (100 mg, 0.43 mmol), pinacol borane **10**,[4] (156 mg, 0.516 mmol), LiOH (30.9 mg, 1.29 mmol) and dichloro 1,1'-bis(diphenylphosphino)ferrocene palladium (II) (35.1 mg, 0.043 mmol) were combined as solids and degassed by evacuating and back filling with nitrogen gas (3 times). DMF (30 mL) was added and the mixture was heated for 2 hr at 100 ºC. Following cooling to rt, EtOAc was added and the mixture was filtered (celite) with EtOAc rinse. The filtrate was washed with water and brine, dried ($MgSO_4$) and concentrated. Silica gel chromatography using a 40-80% EtOAc/heptanes gradient afforded 102 mg (64%) of title compound as a light brown solid. LCMS m/z 373.1 (M+1); ^{1}H NMR ($CDCl_3$, 400 MHz): δ 8.39 (d, *J* = 5.5, 1H), 7.52 (s, 1H), 7.5 (dd, *J* = 8.6, 5.5, 2H), 6.99-7.03 (m, 3H),

4.68 (br s, 2H), 4.39 (br s, 2H), 3.99 (s, 3H), 3.16 (s, 3H). HRMS: calcd for $C_{18}H_{17}FN_4O_2S$ 373.1129 $(M + H)^+$, found 373.1128.

4-(3-(4-Fluorophenyl)-1-methyl-1H-pyrazol-4-yl)isoindoline (22). A mixture of **21** (1.40g, 3.76 mmol) in 48% aq. hydrobromic acid (15 mL) and glacial acetic acid (15 mL) was refluxed for 18h, After cooling to rt, the mixture was diluted with water (10ml) and brought to pH ~12 with 1N aq. NaOH. The aqueous was extracted into 3:1 chloroform/isopropyl alcohol (4 x 50 ml), dried over anh. Na_2SO_4, filtered and concentrated. The crude product was purified by chromatography (ISCO 220 g, 2M ammonia in methanol in methylene chloride from 0% to 10%). Pure product fractions were combined, concentrated and recrystallized from methyl-*t*-butylether to yield 696 mg (62.9%) of title compound as a gray solid. LCMS m/z 295.4 (M+1); ^{1}H NMR ($CDCl_3$, 400 MHz): δ 8.29 (d, J = 5.07, 1H), 7.44 (s, 1H), 7.31-7.39 (m, 2H), 6.93-7.04 (m, 2H), 6.90 (d, J = 5.07, 1H), 4.23 (s, 2H), 3.96 (s, 3H), 3.93 (s, 2H), 2.25 (s, 1H). HRMS: calcd for $C_{17}H_{15}FN_4$ 295.1354 $(M + H)^+$, found 295.1348.

4-(3-(4-Fluorophenyl)-1-methyl-1H-pyrazol-4-yl)-2-methylisoindoline (6). Sodium triacetoxyborohydride (639 mg, 3.02 mmol) was added to a solution of **22** (222 mg, 0.754 mmol) and 37% aqueous formaldehyde solution (0.12 mL, 1.55 mmol) in methylene chloride (5 mL). After stirring at rt for 20 min, the mixture was concentrated and the residue was partitioned between EtOAc and sat $NaHCO_3$, the organics were washed with brine, dried ($MgSO_4$) and treated with decolorizing carbon, filtered (celite) and concentrated to yield 171 mg (73%) of a light yellow glassy solid. ^{1}H NMR ($CDCl_3$, 400 MHz): δ 8.29 (d, J = 5.1, 1H), 7.45 (s, 1H), 7.40 (dd, J = 9.0, 5.5, 2H), 7.02 (dd, J = 9.0, 9.0, 2H), 6.91 (d, J = 5.1, 1H), 4.00 (s, 3H), 3.98 (s, 2H), 3.69 (s, 2H), 2.54 (s, 3H). ^{13}C NMR ($CDCl_3$, 100 MHz): δ 162.55 (d, J_{F-C} = 248.0), 162.5,

148.6, 148.0, 135.9, 132.2, 130.7, 129.5 (d, J_{F-C} = 8.1), 129.0 (d, J_{F-C} =2.9), 122.0, 116.2, 115.4 (d, J_{F-C} = 21.3), 61.6, 59.1, 42.4, 39.1. HRMS: calcd for $C_{18}H_{17}FN_4$ 309.1510 $(M + H)^+$, found 309.1514.

[^{3}H]-9 Preparation. A sealed ampule containing a solution of tritiated methyl iodide (500 mCi, 80 Ci/mmol, 6.3 μmol) in 0.5 mL of DMF was cooled in an ice-bath, opened and placed under positive nitrogen pressure. A solution of **8** (5.3 mg, 17.2 μmol, 2.7 eq) in 0.5 mL of DMF was added followed by solid cesium carbonate (8 mg, 24.6 μmol, 3.9 eq). The ice bath was removed and the reaction mixture was stirred at room temperature for 4 hours. The reaction was quenched by addition of 0.5 mL of water and 1 mL of brine, and the resulting solution was extracted with 3 x 4 mL of EtOAc. The combined organic layers were concentrated in vacuo to yield 35 mCi of non-volatile radioactivity that contained low radiochemical purity [3H]-**9**. 22 mCi of this crude product was purified by reverse phase HPLC according to the following method: Column:Luna C18, 5 μm, 2.0 x 50 mm, Column temperature: ambient, Mobile phase A: 0.1% formic acid in H2O, Mobile phase B: AcN, Injection volume, solvent: 20 μL, can, Gradient: 0 min 15% B, 1 min 15% B, 8 min 60% B, 8.1 min 15% B, Run time: 12 min, Detection: 210 nm. Desired product fractions were combined and concentrated to yield 4.8 mCi of >98% radiochemical purity [3H]-**9**. Product specific activity was determined to be 70.7 Ci/mmol by mass spectrometry.

CK1δ/ε Enzyme Cell Free (Biochemical Assay). The CK1δ and CK1ε kinase assays were performed in a 20 μl final volume in buffer containing 50 mM Tris, pH 7.5, 10 mM $MgCl_2$, 1 mM DTT, 100 μg/mL BSA, 1 mM TCEP, 1.25% Glycerol, 0.0125% P104, 2.5 mM KCl, 10 μM ATP, and 42 μM peptide substrate PLSRTLpSVASLPGL (Flotow et al.,1990). The final

enzyme concentrations were 2 nM for CK1δ and 2.5 nM for CK1ε. Assays were run in a panel format in the presence of 1 μL of compounds or 4% DMSO. The reactions were incubated for 60 min at 25°C for CK1δ and 85 min at 25°C for CK1ε, followed by detection with use of 20 μL of Kinase-Glo Plus Assay reagent according to the manufacturer's instructions. Luminescent output was measured on the Perkin-Elmer Envision plate reader.

CK1δ/ε Whole Cell – WCA (Translocation Assay). COS-7 cells were maintained at 37°C in 5% CO_2 in Dulbecco's Modified Eagle Medium (DMEM) supplemented with 10% fetal bovine serum. Log-phase cells were dislodged with 5-minute treatment of TrypLE Express and viable cell count was determined with Cedex cell counter. Cells were diluted in DMEM medium to a density of 1.5E5 viable cells/mL in 2/3 of the final volume of final transfected cell mix. Cells were cotransfected with two plasmid DNAs, mPER3-GFP in pd2EGFP-N1 vector and human CK1 in pcDNA4/hisA vector (for CK1ε at a ratio of 1:5 respectively for CK1δ at a ratio of 1:11 respectively), using Lipofectamine 2000 reagent according to the manufacturer's recommendations. The transfection mix contained approximately 0.83 ug/mL of DNA and 6 uL/mL of Lipofectamine 2000, in a total of 1/3 of the final transfection volume in Opti-MEM medium. After 20 min at room temperature, the cell mix was combined with the DNA transfection mix, per manufacturer instructions. Transfected cell suspension (50 mL) was dispensed per well by multidrop dispenser into Greiner 384-well Cellcoat (PDL) plates. Compounds were diluted with Opti-MEM I to a 4X concentration before addition to plated cells. Inhibitors of CK1δ/ε were tested at a 11 concentrations to evaluate their ability to inhibit mPER3-GFP translocation to the nucleus. After overnight exposure at 37°C in a CO_2 incubator, cells were fixed by the addition of 12% paraformaldehyde in phosphate-buffered saline (PBS) with 20% sucrose to a final concentration of 4%, and then the cells were incubated for 30 min at

room temperature. The fixative was removed, and cells were washed with PBS and then stained with 0.4 μg/ml Hoechst dye in blocking buffer containing 4% goat serum and 0.1% TritonX for 1 hour. In some experiments, GFP enhancing antibodies were used when needed for signal amplification. Cells were washed again with PBS and stored at 4°C in PBS or scanned immediately with the Cellomics ArrayScan VTI.

Animals

All procedures involving animals were conducted with the approval of the Pfizer Institutional Animal Care and Use Committee. Male C57BL/6J mice from Jackson Laboratories, 9-12 weeks of age, were housed on a 12 hour light/dark cycle and given food and water ad libitum. Animals were allowed to acclimate for 5 days after arrival and were always used within 10 days of arrival.

[^{3}H]-9 Preparation. [^{3}H]-**9** was prepared by the Pfizer Radiochemical Synthesis Group in Groton, CT. Studies were performed using lot 00703442-029-rvc001, 70.7 Ci/mmol, 0.770 mCi/mL in ethanol. The [^{3}H]-**9** dosing solution was prepared by diluting the appropriate amount of stock solution in 0.9% saline to achieve a 100 μCi/mL solution.

Dosing. Mice received a 10 mL/kg subcutaneous (s.c.) injection of PF-670462 at 30 minutes prior to euthanasia. They then received a 3 mL/kg intraorbital injection of [^{3}H]-**9** at 1 minute prior to euthanasia. PF-670462 (100 mg/kg, s.c.) was used to determine the level of non-specific binding. Note that all doses were corrected for salt content of the drug.

[^{3}H]-9 Saturation Binding Procedure. Homogenized hypothalamus was added to assay buffer (50 mM Tris, 2 mM MgCl2, pH 7.4, 20 mg/ml) and incubated with twelve different concentrations of [^{3}H]-**9** at 4 °C for 30 min. The reaction was terminated by rapid filtration through 0.5% PEI soaked GF/B filters using a 96-well Brandel harvester. The filters were

washed 3 times with ice-cold 50 mM TRIS, pH 7.4. The activity of homogenate was measured as total binding (TB). TB (enzyme + radioligand), non-specific binding NSB (receptor + radioligand + excess PF-670462), and specific binding (SB) (SB=TB-NSB) were measured at various radioligand concentrations.

[^{3}H]-9 In Vivo Binding Procedure. Mice were euthanized by live decapitation 30 minutes after dosing and brains removed. Hypothalamus were rapidly dissected and homogenized for approximately 3 seconds each using a polytron at its highest setting (5-6) in 10 volumes (100 mg/mL) of ice-cold assay buffer (50 mM Tris, 2 mM MgCl2, pH 7.4). Two replicates (200 μL each) of the resulting homogenates were filtered using a vacuum manifold apparatus with 25 mm Whatman GF/B filters presoaked in 0.3% polyethyleneimine (PEI). The filters were soaked overnight in 10 mL of Biosafe scintillation fluid. The samples were then counted on a liquid scintillation counter. The unused portions of the brains were frozen on dry ice and reserved for drug exposure analysis.

Target Occupancy Data Analysis. The average total binding of [^{3}H]-**9** detected in hypothalamus tissue was calculated from duplicate determinations of each sample. Specific binding was then calculated by subtracting the average total binding in the presence of the non-specific ligand, PF-670462, from the average total binding. Next, the percent inhibition of specific binding was calculated for each sample where vehicle treatment equaled 100% specific binding (0% inhibition). Drug exposure and binding data for each animal were then plotted as the free drug concentration in brain versus the percent inhibition of specific binding. In order to determine the free brain concentration required to inhibit 50% of the radioligand binding (EC_{50}) curve fitting analysis was performed using proprietary software (Labstats version 3.4 an internal Pfizer application for Excel using a One-site binding model Emax fixed to 100%).

Circadian Rhythm Study Design. Wildtype male mice (C57BL/6J) were singly housed in Nalgene wheel cages which were placed inside isolation boxes, 4 cages per box. Animals were maintained in LD12:12 and baseline data was recorded for ~10 days. Groups of 6 were randomly chosen across boxes for dosing. All dosing was done subcutaneously in DD. The lights were turned off after the baseline period and dosing began the first full day of DD. Animals were dosed for 3 days at circadian time 11 (CT11), which is one hour before activity onset. Animals were kept in DD for 7 days after dosing was completed.

Data Collection & Analysis. Gross motor activity and body temperature data were measured for each animal using an intraperitoneal transmitter. Raw data was imported into ClockLab for analysis. The daily rise in temperature coinciding with activity onset was determined for each day of the study. This method involved scaling the temperature data to better visualize the daily rise. Tau was measured by calculating a regression line through 7 days of daily temperature rise for pre-dosing (LD) and post-dosing (DD). ClockLab calculated the difference between these two regression lines in hours and the phase shift was back-calculated to the first day in DD. One-way ANOVA with Tukey's post-test was used to analyze phase shifts.

Supporting Information

Table 1s: kinase promiscuity panel data, 1H and 13C spectra. This material is available free of charge via the Internet at http://pubs.acs.org.

AUTHOR INFORMATION

Corresponding Author

*Tel: 857-225-2840. Fax 860-686-6052. E-mail: travis.t.wager@pfizer.com.

Notes

The authors declare no competing financial interest.

Acknowledgment

The authors thank Blossom Sneed, Jessica Adams, Dave Rubitski, and Dave Gebhard for CK1i enzyme and whole cell screening efforts and Mark Tibbetts for reagent provision. The authors thank Nandell Keene and Vanessa Paradis and the Pfizer Research and Development and Neuroscience Medicinal Chemistry group for synthesis, scale-up efforts. Lastly, we would like to thank Bethany Kormos for the rendering of the X-ray structure of **9** bound to CK1δ.

Author Contributions

TTW, LZ, SM, SC, AD, CC, KF, SG designed the study. PG, RYC, TWB, JL, SL, ACD, JRH, MM, KS acquired the data. TTW, PG, RYC, TWB, JL, LZ, SC, SL, ACD, CC, KF, SG, JRH, MM and KS analyzed and interpreted the data. TTW, PG, TWB, JL, LZ, SM, CC, KF, SG, JRH, KS drafted the manuscript.

Funding Source: Pfizer Inc

References

(1) Morgan, P., Van Der Graaf, P. H., Arrowsmith, J., Feltner, D. E., Drummond, K. S., Wegner, C. D., and Street, S. D. (2012) Can the flow of medicines be improved? Fundamental pharmacokinetic and pharmacological principles toward improving Phase II survival, *Drug Discovery Today 17*, 419-424.

(2) Zhang, L., Villalobos, A., Beck, E. M., Bocan, T., Chappie, T. A., Chen, L., Grimwood, S., Heck, S. D., Helal, C. J., Hou, X., Humphrey, J. M., Lu, J., Skaddan, M. B., McCarthy, T. J., Verhoest, P. R., Wager, T. T., and Zasadny, K. (2013) Design and Selection Parameters to Accelerate the Discovery of Novel Central Nervous System Positron Emission Tomography (PET) Ligands and Their Application in the Development of a Novel Phosphodiesterase 2A PET Ligand, *J. Med. Chem. 56*, 4568-4579.

(3) Patel, S., and Gibson, R. (2008) In vivo site-directed radiotracers: a mini-review, *Nucl. Med. Biol. 35*, 805-815.

(4) Mente, S., Arnold, E., Butler, T., Chakrapani, S., Chandrasekaran, R., Cherry, K., DiRico, K., Doran, A., Fisher, K., and Galatsis, P. (2013) Ligand–Protein Interactions of Selective Casein Kinase 1δ Inhibitors, *J. Med. Chem. 56*, 6819-6828.

(5) Wager, T. T., Chandrasekaran, R. Y., Hou, X., Troutman, M. D., Verhoest, P. R., Villalobos, A., and Will, Y. (2010) Defining Desirable Central Nervous System Drug Space through the Alignment of Molecular Properties, in Vitro ADME, and Safety Attributes, *ACS Chem. Neurosci. 1*, 420-434.

(6) Wager, T. T., Hou, X., Verhoest, P. R., and Villalobos, A. (2010) Moving beyond rules: The development of a central nervous system multiparameter optimization (CNS MPO) approach to enable alignment of druglike properties, *ACS Chem. Neurosci. 1*, 435-449.

(7) Wager, T. T., Hou, X., Verhoest, P. R., and Villalobos, A. (2016) Central Nervous System Multiparameter Optimization Desirability: Application in Drug Discovery, *ACS Chem. Neurosci.*

(8) Fitzgerald, C. E., Patel, S. B., Becker, J. W., Cameron, P. M., Zaller, D., Pikounis, V. B., O'Keefe, S. J., and Scapin, G. (2003) Structural basis for p38[alpha] MAP kinase quinazolinone and pyridol-pyrimidine inhibitor specificity, *Nat. Struct. Mol. Biol. 10*, 764-769.

(9) Bojnik, E., Farkas, J., Magyar, A., Tömböly, C., Güçlü, Ü., Gündüz, Ö., Borsodi, A., Corbani, M., and Benyhe, S. (2009) Selective and high affinity labeling of neuronal and recombinant nociceptin receptors with the hexapeptide radioprobe [3H]Ac-RYYRIK-ol, *Neurochem. Int. 55*, 458-466.

(10) Meng, Q.-J., Maywood, E. S., Bechtold, D. A., Lu, W.-Q., Li, J., Gibbs, J. E., Dupré, S. M., Chesham, J. E., Rajamohan, F., Knafels, J., Sneed, B., Zawadzke, L. E., Ohren, J. F., Walton, K. M., Wager, T. T., Hastings, M. H., and Loudon, A. S. I. (2010) Entrainment of disrupted circadian behavior through inhibition of casein kinase 1 (CK1) enzymes, *Proc. Natl. Acad. Sci. U.S.A. 107*, 15240-15245.

(11) Badura, L., Swanson, T., Adamowicz, W., Adams, J., Cianfrogna, J., Fisher, K., Holland, J., Kleiman, R., Nelson, F., Reynolds, L., St. Germain, K., Schaeffer, E., Tate, B., and Sprouse, J. (2007) An Inhibitor of Casein Kinase Iϵ Induces Phase Delays in Circadian Rhythms under Free-Running and Entrained Conditions, *Journal of Pharmacology and Experimental Therapeutics 322*, 730-738.

Graphical Abstract: To enable the clinical development of our CNS casein kinase 1 delta/epsilon (CK1δ/ε) inhibitor project we investigated the possibility of developing a CNS positron emission tomography (PET) radioligand. For this effort, we focused our design and synthesis efforts on the initial CK1δ/ε inhibitor HTS hits with the goal of identifying a compound that would fulfill a set of recommended PET ligand criteria. We identified [^{3}H]PF-5236216 (**9**) as a tool ligand that meets most of the key CNS PET attributes including high CNS MPO PET desirability score and kinase selectivity, CNS penetration and low non-specific binding. We further used [^{3}H]-**9** to determine the binding affinity for PF-670462, a literature

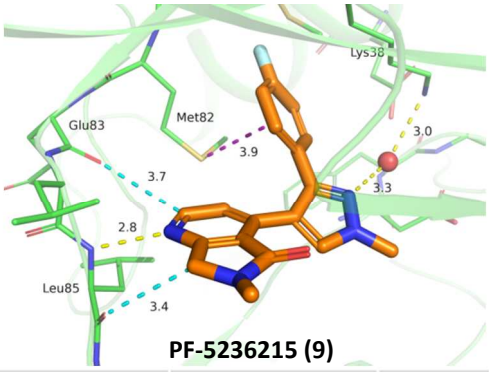

PF-5236215 (9)

Attribute	Target Value	Value
PET MPO	>3	5.5
$C_{b,u}/C_{p,u}$	≥ 0.3	0.7
$F_{u,b}$ and $F_{u,p}$	≥ 0.05	>0.2
B_{max}/K_d	≥ 10x	2.2

CK1δ/ε inhibitor tool compound. Lastly, [^{3}H]-**9** was used to measure in vivo target occupancy (TO) of PF-670462 in mouse and correlated TO with CK1δ/ε in vivo pharmacology (circadian rhythm modulation).

Graphical Abstact (1.375 inches high x 3.5 inches)

PET Ligand Design Criteria

Attribute	Target Value	Value
PET MPO	>3	5.5
$C_{b,u}/C_{p,u}$	≥ 0.3	0.7
$F_{u,b}$ and $F_{u,p}$	≥ 0.05	>0.2
B_{max}/K_d	≥ 10x	2.2

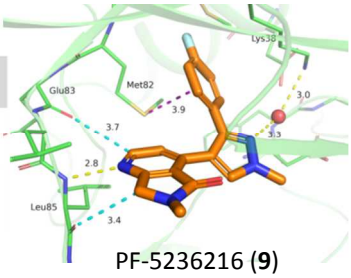

PF-5236216 (**9**)

Identification and Profiling of a Selective and Brain Penetrant Radioligand for In Vivo Target Occupancy Measurement of Casein Kinase 1 (CK1) Inhibitors

*Paul Galatsis, Ramalakshmi Y. Chandrasekaran, Todd W. Butler, Jianke Li, Lei Zhang, Scot Mente, Chakrapani Subramanyam, Shenping Liu, Angela C. Doran, Cheng Chang, Katherine Fisher, Sarah Grimwood, Joseph R. Hedde, Michael Marconi, Klaas Schildknegt, Travis T. Wager**

Abstract: To enable the clinical development of our CNS casein kinase 1 delta/epsilon (CK1δ/ε) inhibitor project we investigated the possibility of developing a CNS positron emission tomography (PET) radioligand. For this effort, we focused our design and synthesis efforts on the initial CK1δ/ε inhibitor HTS hits with the goal of identifying a compound that would fulfill a set of recommended PET ligand criteria. We identified [^{3}H]PF-5236216 (**9**) as a tool ligand that meets most of the key CNS PET attributes including high CNS MPO PET desirability score and kinase selectivity, CNS penetration and low non-specific binding. We further used [^{3}H]-**9** to determine the binding affinity for PF-670462, a literature CK1δ/ε inhibitor tool compound. Lastly, [^{3}H]-**9** was used to measure in vivo target occupancy (TO) of PF-670462 in mouse and correlated TO with CK1δ/ε in vivo pharmacology (circadian rhythm modulation).

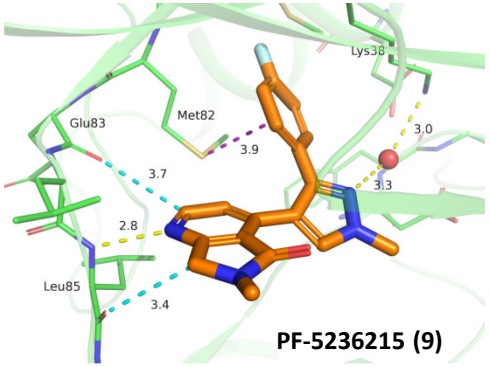

PF-5236215 (9)

Attribute	Target Value	Value
PET MPO	>3	5.5
$C_{b,u}/C_{p,u}$	≥ 0.3	0.7
$F_{u,b}$ and $F_{u,p}$	≥ 0.05	>0.2
B_{max}/K_d	≥ 10x	2.2

Table 1. SAR for CK1 enzyme and whole cell and p38 enzyme

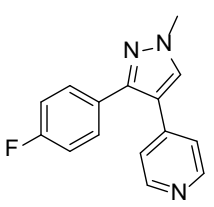

1

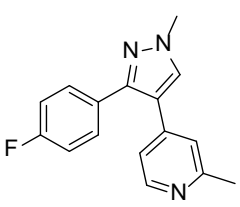

2

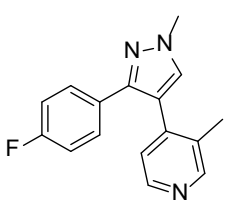

3

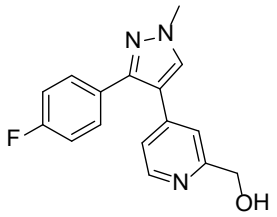

4

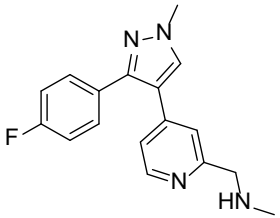

5

Cmpd	CNS MPO (PET MPO) [a]	hCK1δ IC_{50} (nM)[b]	hCK1ε IC_{50} (nM)[b]	hCK1δ EC_{50} (nM)[c]	hCK1ε EC_{50} (nM)[c]	p38 IC_{50} (nM)	P38/ CK1δ
1	4.8 (5.0)	27 (20-35)	126 (107-149)	143 (99-208)	1068 (708-1611)	127 (60-269)	5
2	4.6 (4.9)	37 (n=2)	164 (137-197)	424 (n=1)	ND	340 (n=1)	9
3	4.5 (5.0)	45 (21-91)	203 (140-294)	488 (n=1)	ND	ND	ND
4	5.3 (5.0)	11 (7-17)	68 (48-96)	135 (90-200)	853 (710-1025)	333 (n=1)	29
5	5.8 (5.6)	15 (11-20)	76 (61-95)	45 (28-71)	308 (218-434)	3040 (n=1)	203

[a]Calculated CNS MPO and CNS PET MPO desirability scores were obtained using the published algorithm (maximum value of 6).[2, 6, 7] [b]Purified human CK1δ and CK1ε in vitro enzymes assays. [c]Human CK1δ and CK1ε mediated PER3 nuclear translocation in cells was measured. Each experiment performed in triplicate, mean S.E.M. and data reported as a mean inhibitory activity with (95% CI) from at least three separate experiments unless otherwise noted.

Scheme 1. Cyclic amine design strategy

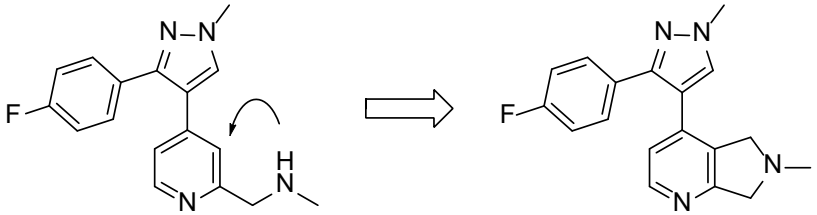

Table 2. SAR for CK1 enzyme and whole cell and p38 enzyme

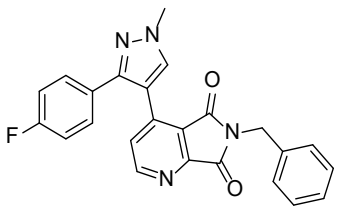

7

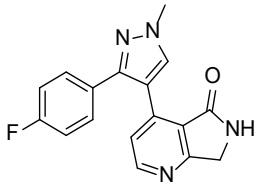

8

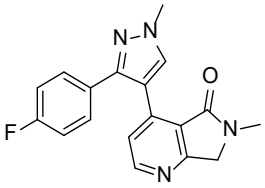

9

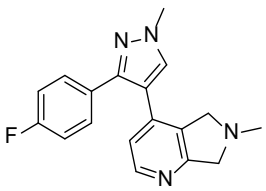

6

Cmpd	CNS MPO (PET MPO) [a]	hCK1δ IC_{50} (nM)[b]	hCK1ε IC_{50} (nM)[c]	hCK1δ EC_{50} (nM)[b]	hCK1ε EC_{50} (nM)[c]	p38 IC_{50} (nM)	P38/ CK1δ
7	4.2 (2.9)	1677 (853-3299)	>4000	>9000	>10000	ND	ND
8	5.8 (5.9)	10 (9-12)	56 (50-64)	107 (93-123)	630 (567-701)	701 (n=2)	70
9 (PF-5236216)	6.0 (5.5)	8 (7-9)	36 (31-43)	58 (49-68)	318 (282-351)	>861	>114
6	5.7 (5.5)	43 (15-118)	232 (113-478)	369 (161-836)	1541 (n=2)	>1884 (n-2)	>44

[a]Calculated CNS MPO and CNS PET MPO desirability scores were obtained using the published algorithm (maximum value of 6).[2, 6, 7] [b]Purified human CK1δ and CK1ε in vitro enzymes assays. [c]Human CK1δ and CK1ε mediated PER3 nuclear translocation in cells was measured. Each experiment performed in triplicate, mean S.E.M. and data reported as a mean inhibitory activity with (95% CI) from at least three separate experiments unless otherwise noted.

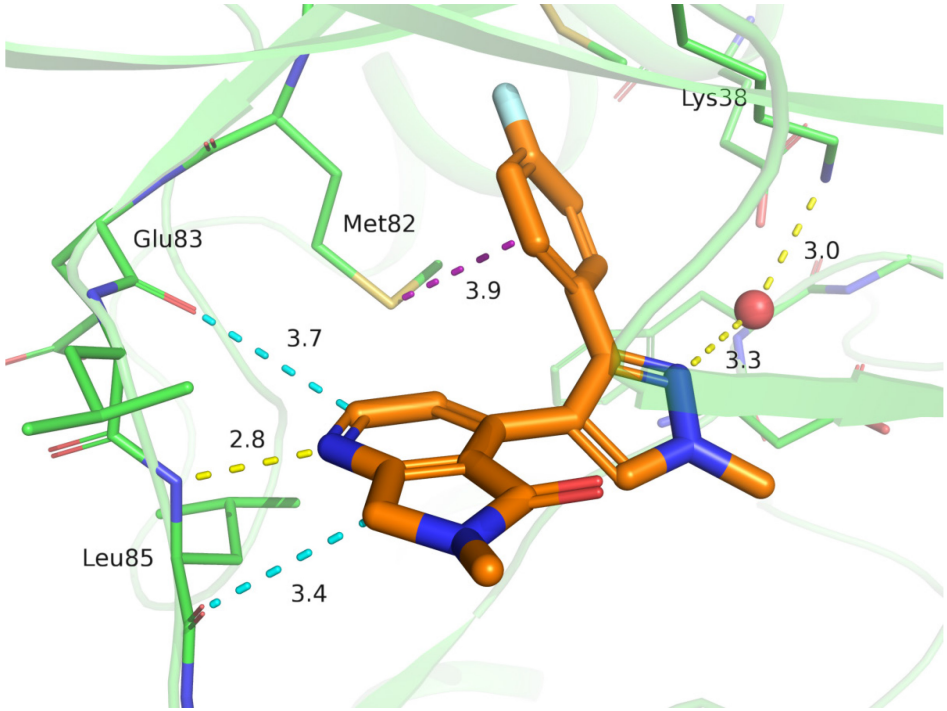

Figure 1. Binding of CK1δ/ε inhibitor **9** to CK1δ.

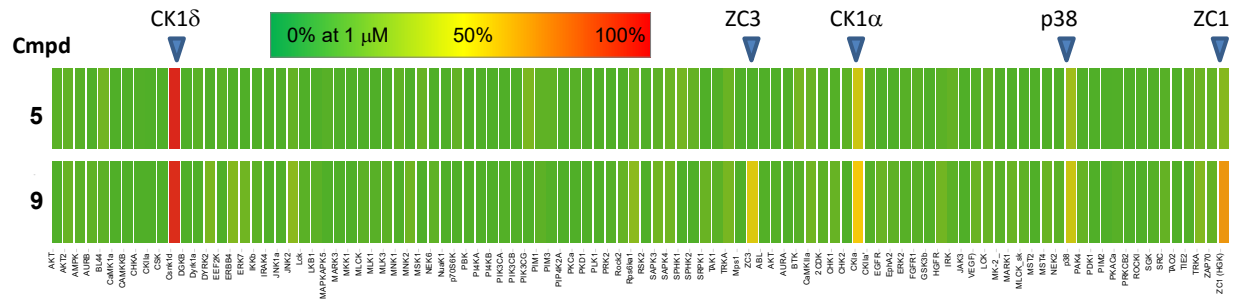

Figure 2. A) Percent inhibition of a 100 kinase target promiscuity panel at 1 μM for compound **5** and **9**. Heat map colors for this continuum: green, 0% inhibition; yellow, 50% inhibition; red, 100% inhibition.

Table 3. Off-target selectivity profiling IC50 format and selectivity[a]

Cmpd	Kinase	IC_{50} (nM)	%Inh (1μM)	Selectivity CK1δ/target
5	CK1α	1059	34	71
5	p38	3040	21	203
5	ZC1	>10000	21	>667
5	ZC3	>10200	-1	>680
9	CK1α	630	51	79
9	p38	861	37	108
9	ZC1	873	65	109
9	ZC3	1573	42	197

[a]IC_{50} determination for the four targets hit in the promiscuity panel with inhibition >30% for compound **9**, along with the matched set for compound **5**.

Table 4. ADME property summary of for **5** and **9**.

Cmpd	HLM[a]	RLM[b]	P_{app}[c]	P-gp[d]	Bcrp[f]	Mouse $F_{u,p}$	Rat $F_{u,b}$	$C_{max,b,u}$ [nM][g]	$AUC_{0-\infty}$ C_b/C_p	$AUC_{0-\infty}$ $C_{b,u}/C_{p,u}$
5	**18**	64.5	17.9	2.2	4.2	0.39	0.09	1480	3.1	0.7
9	**<9**	<39	30	1.2	1.9	0.38	0.24	8685	0.7	0.7

[a]Human liver microsomal clearance (mL/min/mg). [b]Rat liver microsomal clearance (mL/min/mg). [c]Passive permeability (P_{app} AB x 10^{-6} cm/sec) determined by RRCK. [d]Borst MDR1 Efflux Ratio (BA/AB). [f]Mouse Bcrp Efflux Ratio (BA/AB). [g]Mouse $C_{max,b,u}$ values are reported as maximum free drug concentration in brain at a 56 mg/kg dose, s.c.

Scheme 2. Synthesis of [^{3}H]-9

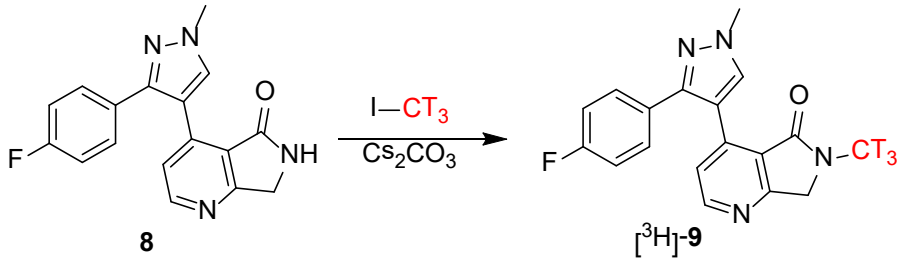

8 [^{3}H]-**9**

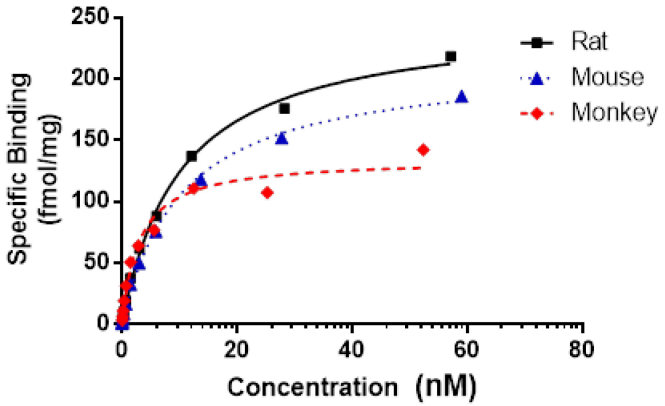

Cmpd	Species	B_{max} (fmol/mg)[a]	B_{max} (nM)[b]	K_d (nM)[a]	B_{max}/K_d
9	Rat	250.2 (236.4-264.9)	12.5	10.2 (8.6-11.7)	1.2
	Mouse	214.2 (198.7-229.6)	10.7	10.4 (8.2-12.6)	1.0
	Monkey	135 (126.0-144.0)	6.7	3.0 (2.3-3.7)	2.2

Figure 3. [a]Saturation [^{3}H]PF-5236216 binding curves for rat, mouse, and monkey brain hypothalamus tissue. Each experiment was performed in triplicate; mean S.E.M. B_{max} and K_d values were determined by GraphPad Prism analyses. [b]B_{max} (fmol/mg) values were converted to nM concentrations assuming 50 mg protein/g wet tissue.[9]

Table 5. CK1i brain receptor occupancy from brain binding techniques in mouse for CP-670462 using [^{3}H]-**9**

Compound	Treatment (mg/kg, sc)	$C_{b,u}$ (nM)	Rat CK1δ/ε IVTO (%)[a]
9	100	1022	100
	10	210	81
	3.2	78	31
	EC_{50}	62 ± 27 nM[b]	

[a]Brain region evaluated: rat hypothalamus (mean ± SEM, n = 3–4). Rat in vivo TO analysis with [^{3}H]-**9** and E_{max} fixed at 100%.

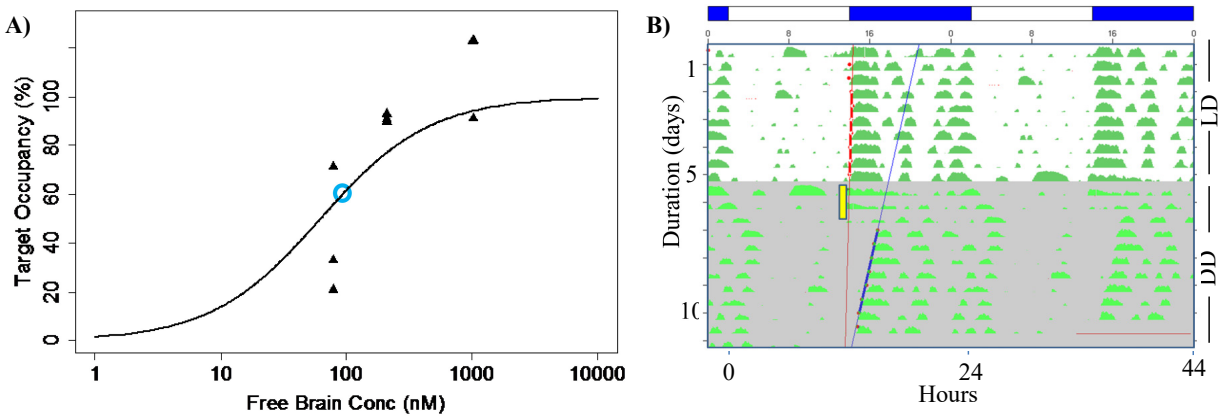

Figure 4. A) Brain region evaluated: rat hypothalamus brain receptor occupancy curves from the in vivo TO protocol in rat. Rat IVTO analysis with [^{3}H]-**9** as tracer and Emax fixed at 100%. The black triangle data points represent actual measured TO and brain PK from individual animals. The solid line is the data-fitted TO model. The blue circle represents exposure, C_{ave} (over 4hrs) and TO (67% IVTO) to yield a 4 hr phase shift in dark: dark (D:D) mouse in vivo circadian rhythm model (32 mg/Kg s.c. after 3-days dosing of PF-670462). B) Representative scaled temperature actograms for PF-670462 reveal significant period lengthening by PF-670462 in WT animals after 3 d of dosing, previously reported. The phase shift depicted was -3.70 hours following dosing for 3 days in DD.

Table 5. Summary of CNS PET attributes for **9.**

Property	Attribute	Target Value	Value[a]	
Physicochemical Properties	PET MPO	>3	5.5	
Synthetic Enabled Label Sites	[^{3}H], [^{11}C], [^{19}F]	1 site	2 sites	
Brain Permeability	P_{app}	> 10	30	
	MDR ER	≤ 2.5	1.2	
	Bcrp ER	≤ 2.5	1.9	
	$C_{b,u}/C_{p,u}$	≥ 0.3	0.7	
Non-specific Binding	$F_{u,p}$	≥ 0.15	0.38	
	$F_{u,b}$	≥ 0.05	0.24	
	$F_{u,b}$ and $F_{u,p}$	≥ 0.05 and ≥ 0.05	Yes	
Pharmacology	Selectivity	>30x	>70x	
	B_{max}/K_d	≥ 10x	2.2	

[a]Color code: red, fail to meet target value and green, meet target value.

Scheme 3. Synthesis of 7, 8, and 9[a]

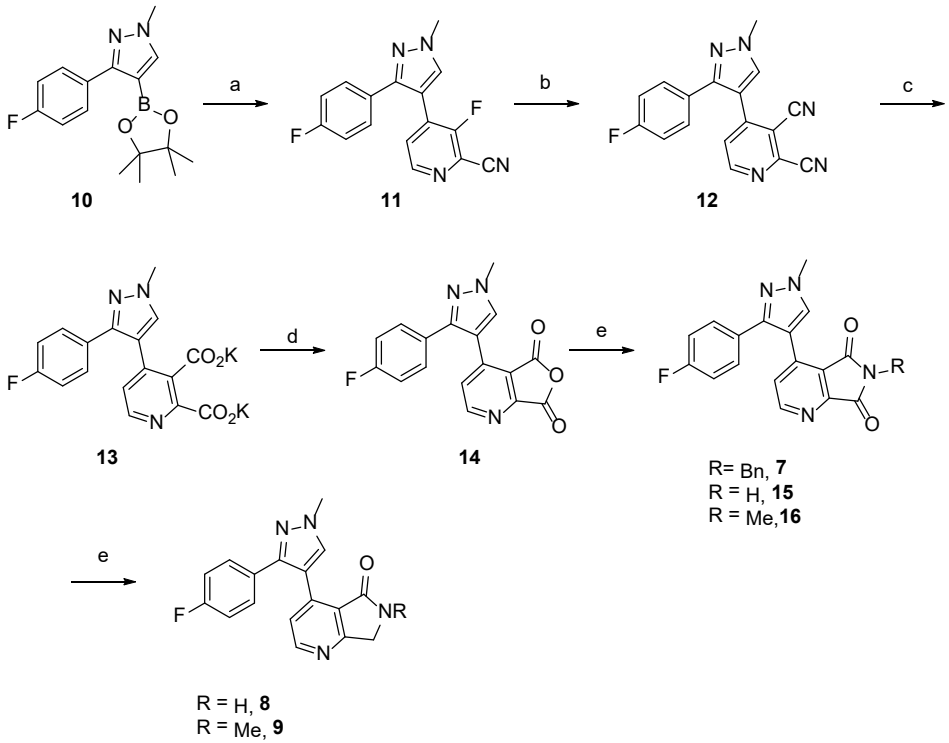

[a]Reagents and Conditions: (a) 3-fluoro-4-iodopicolinonitrile, 1.2 equiv of Cs_2CO_3, DMF, $Pd^2(dba)_3$, 50 °C, 6 h (59%); (b) KCN, DMSO, 50 °C, 2 h (quant.); (c) 5N aq KOH, 100 °C, 24 h (88%); (d) Ac_2O, HOAc, THF, 110 °C, 3 h; (e) Ac_2O, HOAc, BnNH2 (**7**, 75%), or NH_4OH (**15**, 92%) or $MeNH_2$ (**16**, 93%), 80-120 °C, 2 h; (f) 5 equiv of Zn dust, HOAc, 110 °C, 1.5-4.5 h, (**8**, 41%),(**9**, 53%)

Scheme 4. Synthesis of 6[a]